

Supporting Information for

GmEID1 modulates light signaling through the Evening Complex to control flowering time and yield in soybean

Chao Qin^{1,7}, Haiyang Li^{2,7}, Shengrui Zhang¹, Xiaoya Lin², Zhiwei Jia³, Fen Zhao^{1,4}, Xiuzhi Wei¹, Yuanchen Jiao¹, Zhuang Li¹, Zhiyuan Niu^{1,5}, Yonggang Zhou⁶, Xiaojiao Li³, Hongyu Li¹, Tao Zhao¹, Jun Liu¹, Haiyan Li⁶, Yuping Lu³, Fanjiang Kong^{2*} and Bin Liu^{1*}

Email: Bin Liu (liubin05@caas.cn) or Fanjiang Kong (kongfj@gzhu.edu.cn).

This PDF file includes:

Supporting text

Figures S1 to S22

SI References

Other supporting materials for this manuscript include the following:

Datasets S1 to S4

1 Supporting Information Text

2 SI Appendix Materials and Methods

3 RNA sequencing and data analysis

4 The W82 cultivar was grown under LD conditions (25°C) in green house for 21 days. The second
5 fully expanded trifoliolate leaves were collected every four hours from the beginning of night for a
6 complete photoperiod of 24 hours. Total RNA was extracted from each sample using TRIzol
7 reagent (TIANGEN). Multiplexed libraries were prepared with Kit (NEB #E7760S) and sequenced
8 using an Illumina platform. Raw reads were filtered to remove adapter sequences using the
9 sequence pre-processing tool Trimmomatic version 0.39, and only reads with quality scores
10 (Phred) R30 were kept for mapping to soybean reference genome (Wm82.a2.v1, V275) using
11 HISAT2 version 2.1.0 with default parameters. The data of gene expression (FPKM) values was
12 listed in **Dataset 1**. The genes with average TPM over 1 were used for further analysis. The
13 Pearson's correlation of expression levels was calculated between *E1* and the other genes using
14 R project. The correlated genes with *p* value less than 0.05 were prioritized in this study. The data
15 of screening of candidate regulators of *E1* is listed in **Dataset 2**.

17 Gene expression analysis

18 To compare the transcript level of target genes in the indicated lines, the plants were grown under
19 LD or SD conditions for 20 days. The second fully expanded trifoliolate leaves were harvested at
20 4-hour (h) intervals during a 24-hour (h) photoperiod. Total RNA was extracted using Trizol
21 Reagent (TIANGEN) and cDNA was synthesized from total RNA treated with DNase (2 µg,
22 reaction total volume of the reaction 10 µl) using a reverse transcription kit (TransGen Biotech).
23 qRT-PCR was performed in 384-well optical plates using a SYBR Green RT-PCR kit (Vazyme)
24 with ABI Q7 equipment. All primers used for indicated genes are listed in **Dataset S3**. Three
25 independent biological replicates were performed, and three replicate reactions were used for
26 each sample.

28 Plasmid construct and plant transformation

29 To generate CRISPR / Cas9 engineered mutants, gRNAs were designed using the CRISPR
30 direct website (<http://crispr.dbcls.jp/>) (1). Multiple target gRNAs were selected for each gene to
31 construct the CRISPR/Cas9 vector according to the protocol reported previously (2). The editing
32 efficiency of each construct was evaluated using the soybean hairy root system (3, 4), and at
33 least two vectors with high editing efficiency for each gene were selected for soybean
34 transformation. To construct the overexpression vectors, the *GmEID1* coding DNA sequence
35 (CDS) was amplified by PCR using cDNA derived from young W82 seedlings, cloned into the
36 Gateway entry vector *pDONR^{Zeo}*, and then cloned into the destination binary vector
37 *pEarleyGate101* or *pEarleyGate104* using the Gateway recombination system (Invitrogen) (5).
38 For *J-HA* overexpression, the CDS of the *J* was amplified by PCR using cDNA derived from W82
39 seedlings. A modified vector based on PTF101 was used to construct the *35S::J-HA* vector. The
40 CRISPR/Cas9 vectors and overexpression vectors mentioned above were individually introduced
41 into the *Agrobacterium tumefaciens* strain EHA105 by electroporation and then transformed into
42 the cultivar TL1 or W82 using the cotyledon-node method (6).

44 Subcellular localization in protoplasts

45 To investigate the subcellular localization of the indicated proteins, the CDS of *GmEID1* was
46 inserted into the *pA7-YFP* vector at the *BamHI* and *SmaI* sites using the In-Fusion system
47 (Clontech) to generate the transient expression constructs of *pA7-GmEID1-YFP* driven by the
48 *35S* promoter. The *pA7-GmMYB29-RFP* construct was used as a nuclear marker as previously
49 described (7). The empty vector *pA7-YFP* was used as a control. The above constructs were
50 transformed into *Arabidopsis* mesophyll protoplasts. The subcellular localization images were
51 captured under a Zeiss LSM980 confocal laser scanning microscope and processed using ZEN
52 2009 Light Edition software.

53

54 **Yeast two-hybrid experiments**

55 The yeast two-hybrid assay was performed according to the manufacturer's instructions (Yeast
56 Handbook Clontech). *GmEID1* CDS were fused in frame with the CDS of the GAL4 DNA binding
57 domain in the *pBridge* bait vector (Clontech). The CDS of the EC (*J*, *GmELF3b-1*, *GmELF3b-2*,
58 *GmELF4a*, *GmELF4b*, *GmLUX1* and *GmLUX2*), *E3* and *E4* were fused in frame with the CDS of
59 the GAL4 transcription activation domain in the prey vector *pGADT7* (Clontech). The bait and
60 prey plasmids were cotransformed into the yeast strain *Saccharomyces cerevisiae* AH109
61 (Clontech). The yeast cells were grown on a minimal medium SD/-Leu-Trp according to the
62 manufacturer's instructions. Positive clones were selected in SD/-Ade-His-Leu-Trp selection
63 medium at 30°C for 3 days to evaluate protein interactions. SD/-Ade-His-Leu-Trp selection
64 medium that added 10 µM PCB which was used to interact with E3/E4 with GmEID1 under red
65 light (30 µmol m⁻² s⁻¹), far-red light (20 µmol m⁻² s⁻¹) and dark conditions.

66
67 For β-galactosidase activity assay, colonies were selected and cultured at 180 rpm, 28°C in the
68 dark until they reached OD600 = 0.1 in a 10 ml flask containing 4 ml of SD medium (-Leu/-Trp). 2
69 mL yeast culture was divided into 8 mL YPDA culture solution and cultured at 160 rpm at 30°C
70 under dark conditions for the interaction of GmEID1 with the EC, and red light (30 µmol m⁻² s⁻¹),
71 Far-red (30 µmol m⁻² s⁻¹) and darkness for the interaction of GmEID1 with E3/E4 until OD600 =
72 0.5-0.8 before the β-galactosidase assay. The relative bait-prey interaction was presented as β-
73 gal units = 1000×OD578/(T×V×OD600), T as response time (min); V = 0.1 × concentration factor.
74 Standard deviations (n = 3) are shown.

75 **Dual-Luciferase assay**

76 For Dual-Luciferase assays in tobacco, the CDS of *GmEID1* was amplified and cloned in the
77 vector *pCAMBIA1300-nLUC*, and the CDS of the EC (*J*, *GmELF3b-1*, *GmELF3b-2*) were
78 amplified and cloned in the vector *pCAMBIA1300-cLUC*. *Agrobacterium tumefaciens* strain
79 GV3101 bacteria carrying different constructs were co-infiltrated into tobacco leaves. After
80 infiltration, tobacco plants were incubated in the dark at 25°C for 12 h and then transferred to far-
81 red light (30 µmol m⁻² s⁻¹) conditions for an additional 36 h before analysis for LUC activity. A
82 low-light-cooled CCD imaging apparatus (Tenon-5200) with GelCap software was used to
83 capture the LUC image. For each analysis, at least eight independent leaves of tobacco leaves
84 were infiltrated and analyzed. To determine the effects of E3 on the interaction of GmEID1 with
85 EC proteins by LCI assays, GV3101 colonies harboring constructs expressing GmEID1-nLUC,
86 cLUC-J and E3-Flag were infiltrated into leaves of tobacco. GUS-Flag was used as a negative
87 control.
88

89 **In-vitro pull-down assay**

90 The full-length CDS of *E3* or *E4* fused with *3xFlag* was cloned into the *pMAL-c5X* vector. The full-
91 length CDS of *J* or *E1* was cloned into the *pET-28a (+)* vector. The His-J and His-E1 recombinant
92 proteins were purified with Ni-NTA (QIAGEN). E3-3xFlag and E4-3xFlag proteins were purified
93 using TnT Quick Coupled Transcription/Translation Systems according to the manufacturer's
94 instructions (Promega, L1170). Holoproteins of E3 and E4 were generated by incubating the
95 respective apoproteins with 20 mM phycocyanobilin (PCB) for 1 h in the dark on ice to allow the
96 incorporation of the chromophore (J&K Scientific, P14137) as previously reported (8). The
97 combination of proteins as indicated were mixed and pull down using Anti-Flag antibody.
98
99

100 **RICE system to investigate J protein levels**

101 The *35S::J-3xFlag* vector was introduced into *A. tumefaciens* strain K599, which was used to
102 infect young seedlings of indicated lines in the hypocotyl region to induce transgenic hairy roots
103 according to a previously reported method (10). Hairy roots induced by Empty K599 were used as
104 the WT control. Callus induction medium (2.22 g/l Murashige & Skoog Basal Medium with
105 Vitamins, 0.59 g/l MES monohydrate, 30 g/l sucrose, 1 mg/l 2, 4-D, 0.1 mg/l 6-BA, 0.1 g/l
106 Timentin) was prepared as previously described (11). The transgenic roots were grown in callus
107 induction medium for 2 weeks under LD or SD conditions. Those transgenic callus lines

108 confirmed by western blot were transferred to a fresh callus induction medium for subculturing. To
109 compare the protein levels of J-Flag in the indicated lines, at least 10 independent transgenic
110 callus lines were used for western blot analysis.

111

112 **Immunoblot Assay**

113 The fresh leaves or callus were collected in liquid nitrogen, ground to fine powder, and
114 homogenized in 4×SDS-PAGE loading buffer [250 mM Tris-HCl pH 6.8, 10% SDS, 50% glycerol,
115 40 mM DTT, and 0.01% Bromophenol blue]. Protein extracts were separated by 10% SDS-
116 PAGE, transferred to PVDF (0.45 µm, Immobilon-P) membrane, and blotted with indicated
117 antibodies. The anti-E3 antibody was raised in a previous study (9).

118

119 **Statistical analysis**

120 Statistical analysis was performed using GraphPad 9.0 and Microsoft EXCEL. All numerical
121 values are presented as Mean values ± SD. The differences between control and treatments
122 were tested using two-tailed Student's t tests and ANOVA with Tukey's post-test.

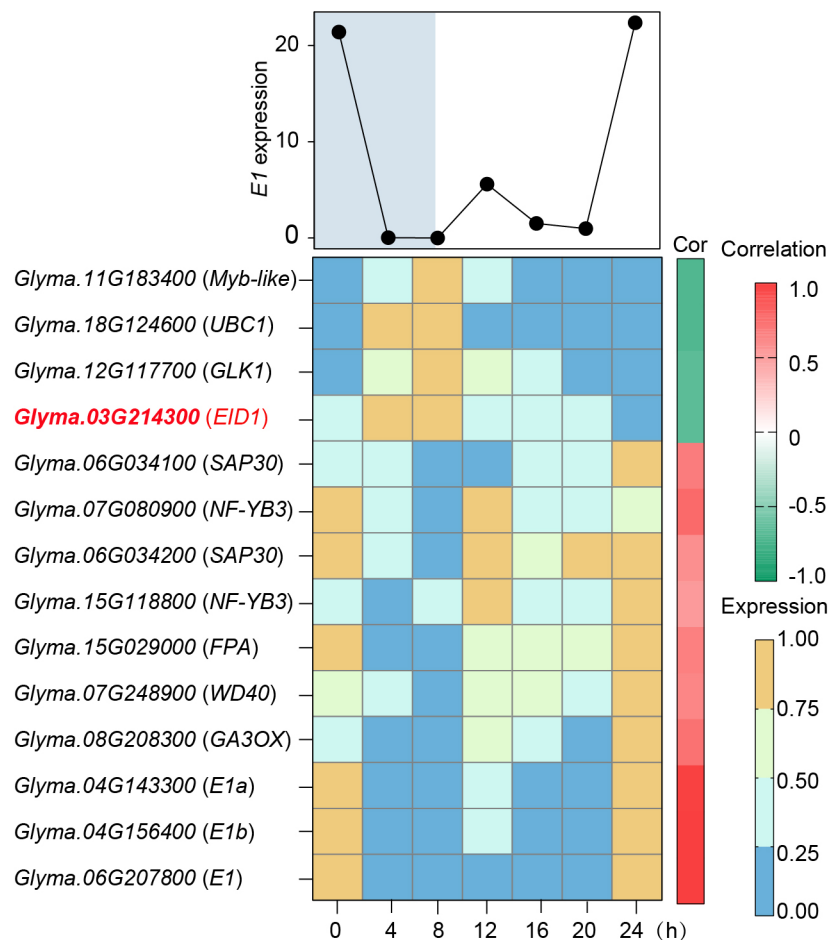
123 **Primers and accession Numbers**

124 All primers used in this study are listed in **Dataset S3**. Gene sequences may be obtained from
125 the Phytozome database (https://phytozome-next.jgi.doe.gov/info/Gmax_Wm82_a2_v1). The
126 accession numbers are *GmEID1* (Glyma.03G214300), *E3* (Glyma.19G224200), *E4*
127 (Glyma.20G090000), *J* (Glyma.04G050200), *GmELF3b-1* (Glyma.14G091900), *GmELF3b-2*
128 (Glyma.17G231600), *GmELF4a* (Glyma.11G229700), *GmELF4b* (Glyma.07G037300), *GmLUX1*
129 (Glyma.12G060200), *GmLUX2* (Glyma.11G136600), *E1* (Glyma.06G207800), *GmFT2a*
130 (Glyma.16G150700), *GmFT5a* (Glyma.16G044100), *GmCCA1a* (Glyma.07G048500), *GmPRR3b*
131 (Glyma.12G073900) and *GmActin* (Glyma.18G290800).

132

133 **Supplemental Figure**

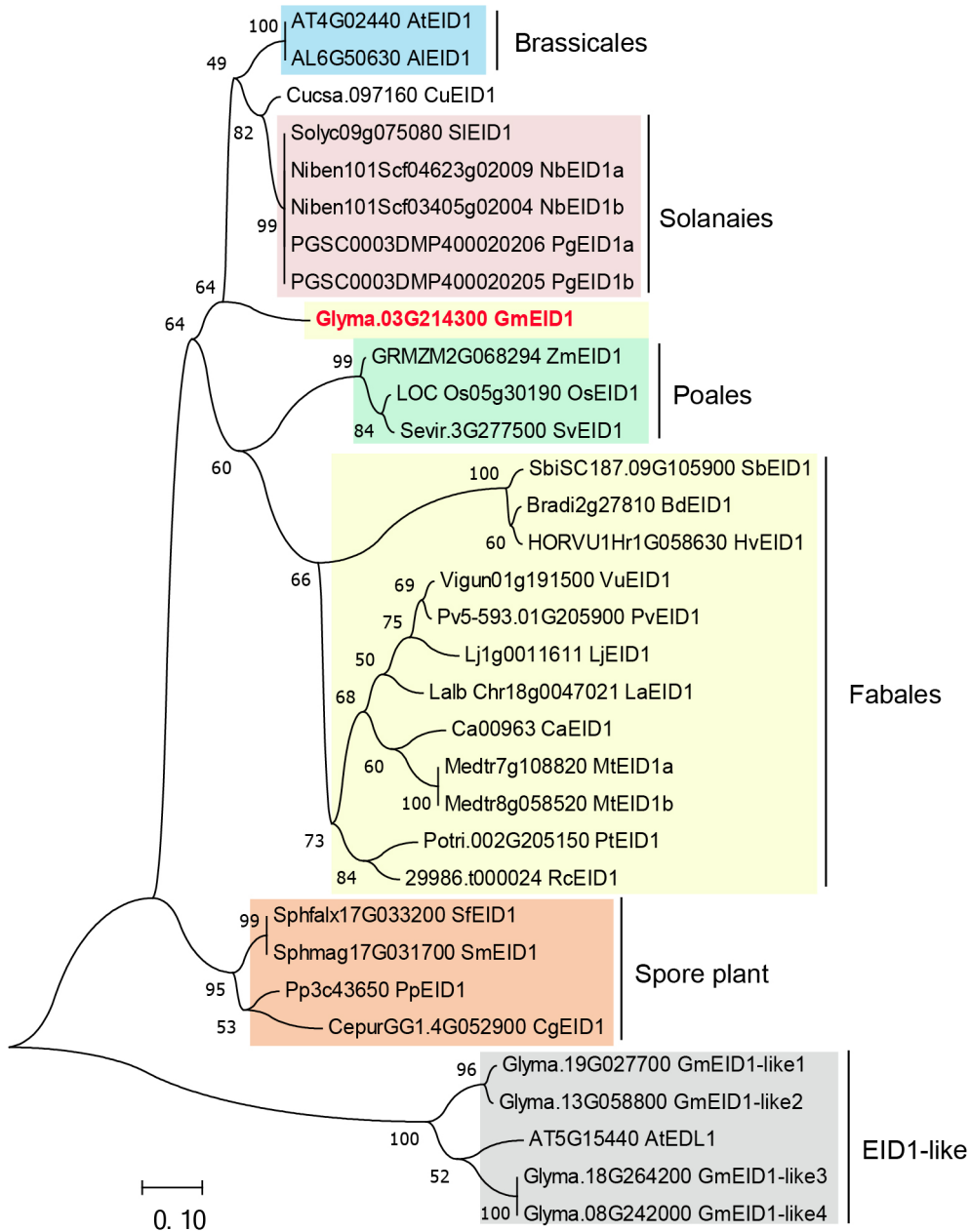
134



135

136

137 **Fig. S1.** Screening of candidate regulators of *E1*. Heat map showing candidate genes with the
 138 same or opposite expression pattern of *E1* during a 24 h photoperiod by transcriptome
 139 sequencing (RNA-seq) using the second trifoliolate leaves of W82 plants grown under LD
 140 conditions. The above color scale bar represents the degree of correlation with the *E1* expression
 141 pattern. The bottom color scale bar represents the relative transcript level of each gene with the
 142 expression peak arbitrarily set to 1. The expression of candidate genes by transcriptome
 143 sequencing are listed in **Datasets S2**.

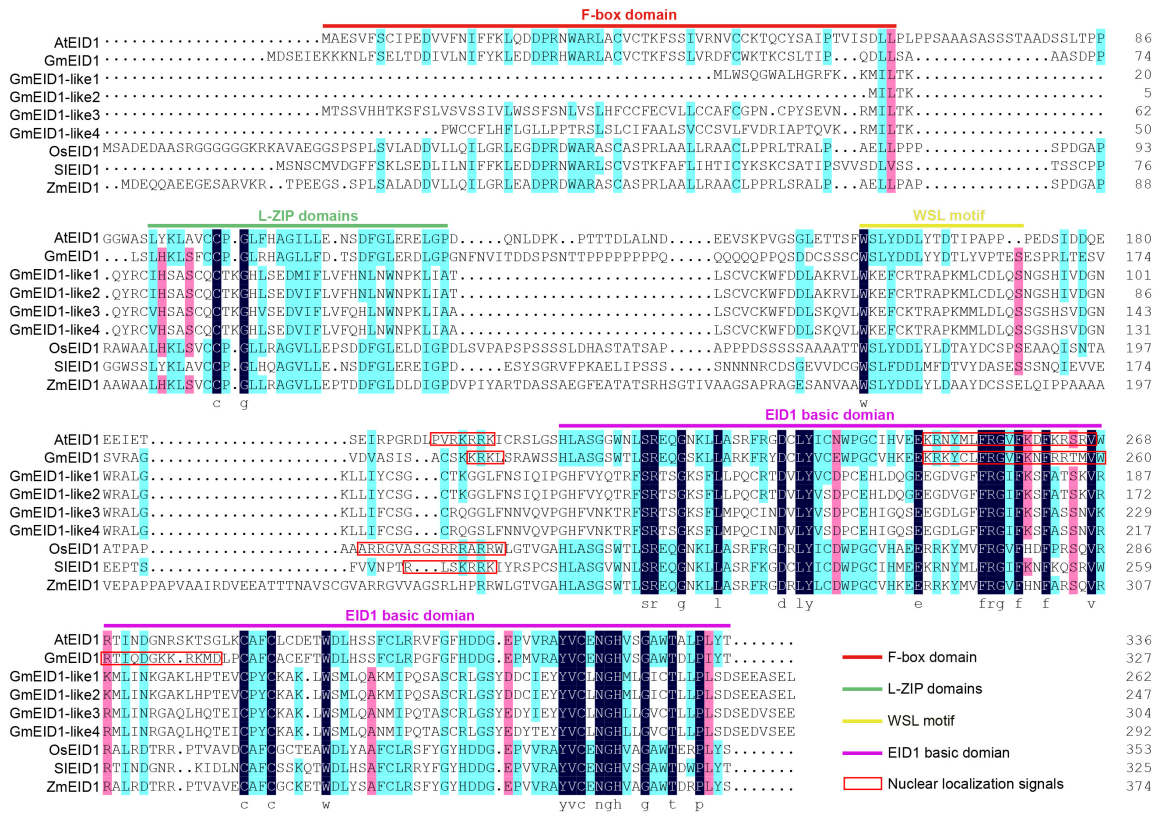


144

145

146 **Fig. S2.** Phylogenetic analysis of EID1 and its homologous proteins in the indicated species. The
 147 tree was constructed using the neighbor-joining method of the MEGA7 software. All protein
 148 sequences are listed in **Dataset S4**.

149

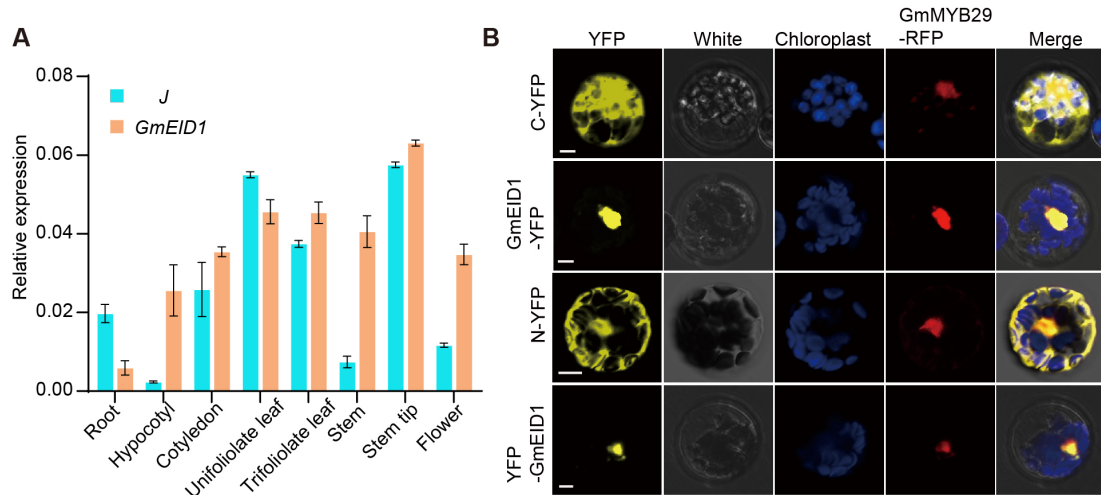


151

152

153 **Fig. S3.** Alignment of EID1 homologous proteins. The protein sequences of EID1 and its
 154 homologs were aligned by ClustalW Multiple alignments in DNAMAN and manually adjusted.
 155 Protein sequences of *Arabidopsis* (AtEID1, AT4G02440), *Glycine max* (GmEID1,
 156 Glyma.03G214300; GmEID1-like1, Glyma.19G027700; GmEID1-like2, Glyma.13G058800;
 157 GmEID1-like3, Glyma.18G264200; GmEID1-like4, Glyma.08G242000), *Oryza sativa* (OsEID1,
 158 LOC_Os05g30190), *S.lycopersicum* (SIEID1, Solyc09g075080), and *Zea mays*L. (ZmEID1,
 159 GRMZM2G068294_T01) were retrieved from Phytozome (<https://phytozome-next.jgi.doe.gov/>).
 160 All protein sequences are listed in **Dataset S4**. The conserved domains were highlighted by
 161 indicated color lines on the top, respectively. Red boxes indicate the nuclear localization signals.

162

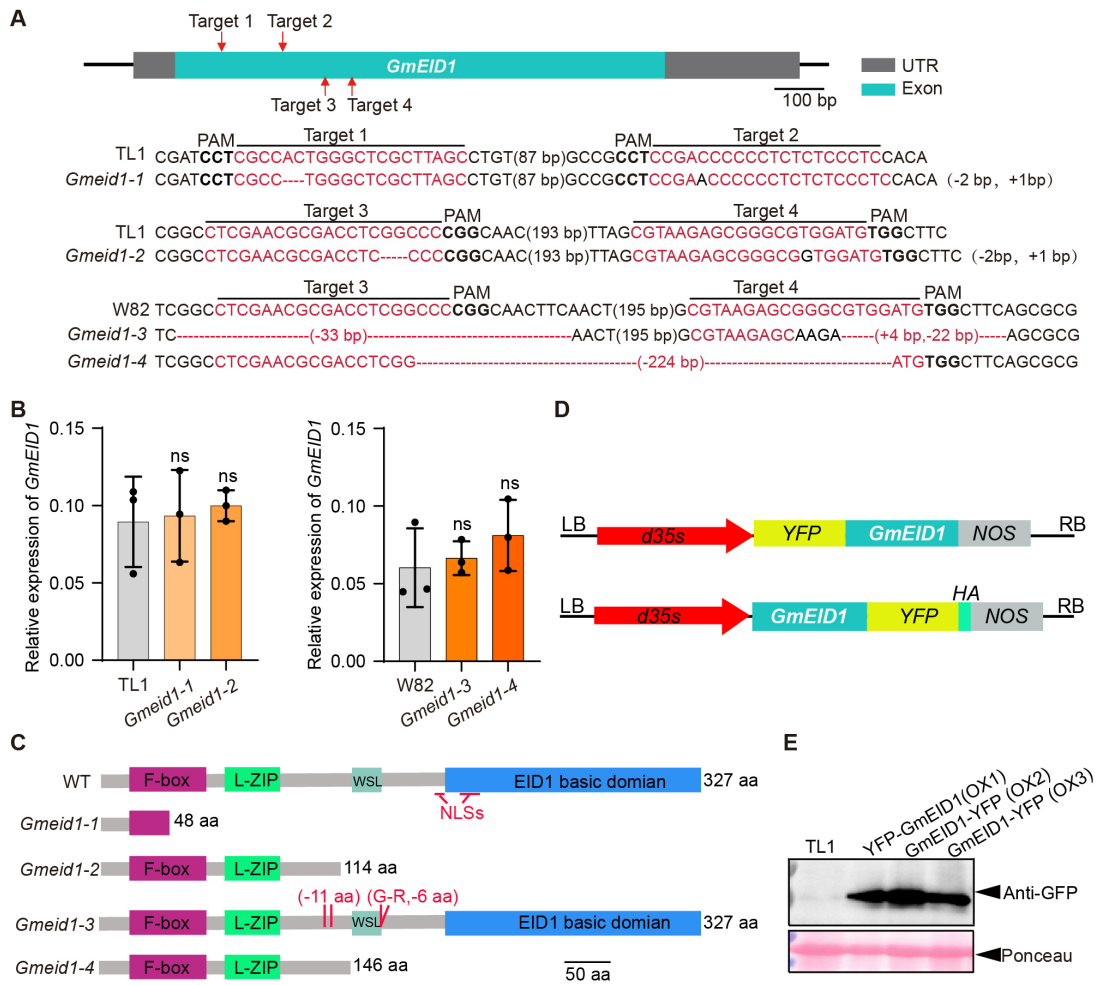


163

164

165 **Fig. S4.** Spatiotemporal expression and subcellular localization of GmEID1 in soybean. (A)
 166 Comparison of transcript levels of the *J* and *GmEID1* genes in the indicated tissues. Root,
 167 hypocotyl, cotyledon, unifoliolate leaf, trifoliolate leaves, stem, stem tip and flower of W82 were
 168 harvested for qRT-PCR analysis. The relative expression level is shown as mean \pm SD ($n = 3$).
 169 The *GmActin* gene was used as an internal control. (B) Subcellular localization of GmEID1-YFP
 170 and YFP-GmEID1 fusion proteins in *Arabidopsis* mesophyll protoplasts. The GmMYB29-RFP
 171 fusion protein was used as a nucleus marker. The YFP protein alone was used as a negative
 172 control. Scale bar, 5 μ m.

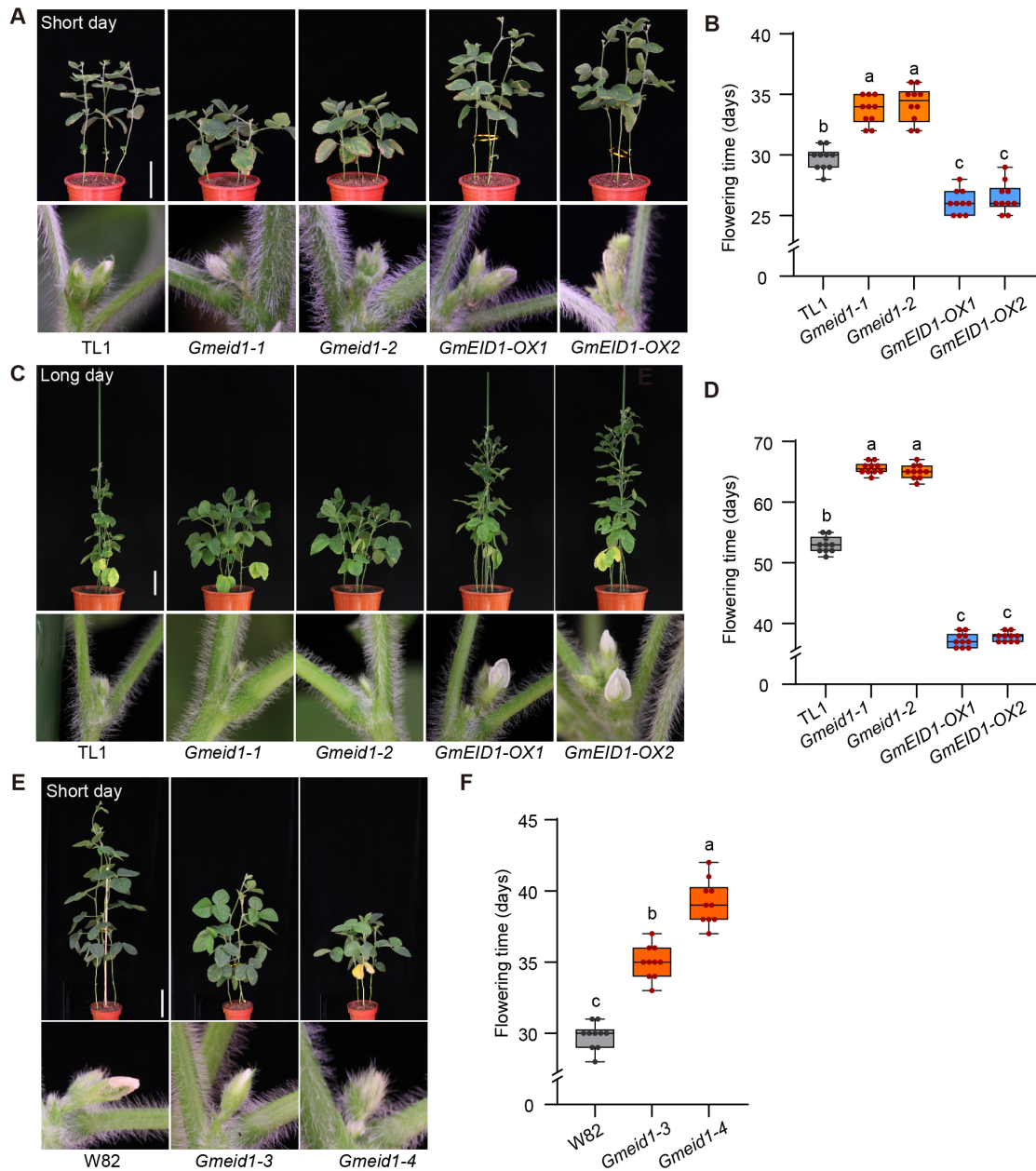
173



175

176

177 **Fig. S5.** Generation of the *Gmeid1* mutants and overexpression lines. (A) Four single-guide
 178 RNAs (red arrows) were designed to target the exon of *GmEID1*. Sequences of representative
 179 homozygous mutants (*Gmeid1-1* and *Gmeid1-2* in TL1 background, *Gmeid1-3* and *Gmeid1-4*
 180 in W82 background) at the T2 generation are shown. The gRNA target sites are highlighted in red
 181 letters with the protospacer-adjacent motif (PAM) in bold. The black-letter and dashed lines within
 182 the target sites denote nucleotide insertion and deletion, respectively. (B) The transcript levels of
 183 the *GmEID1* genes in indicated lines grown under LD conditions. The first trifoliolate leaves at ZT4
 184 were collected for qRT-PCR analysis. Mean values \pm SD ($n = 3$) is shown. *GmActin* was used
 185 as an internal control. (C) Schematic diagram showing the intact and mutated GmEID1 proteins in
 186 *Gmeid1* mutants as in (A). (D) Schematic diagram showing the YFP-GmEID1 or GmEID1-YFP
 187 overexpression construct. (E) Immunoblot showing the expression of YFP-GmEID1 and GmEID1-
 188 YFP fusion proteins in the transgenic plants using anti-GFP antibody. The wild-type TL1 sample
 189 was used as the negative control. The ponceau band was used as the loading control.

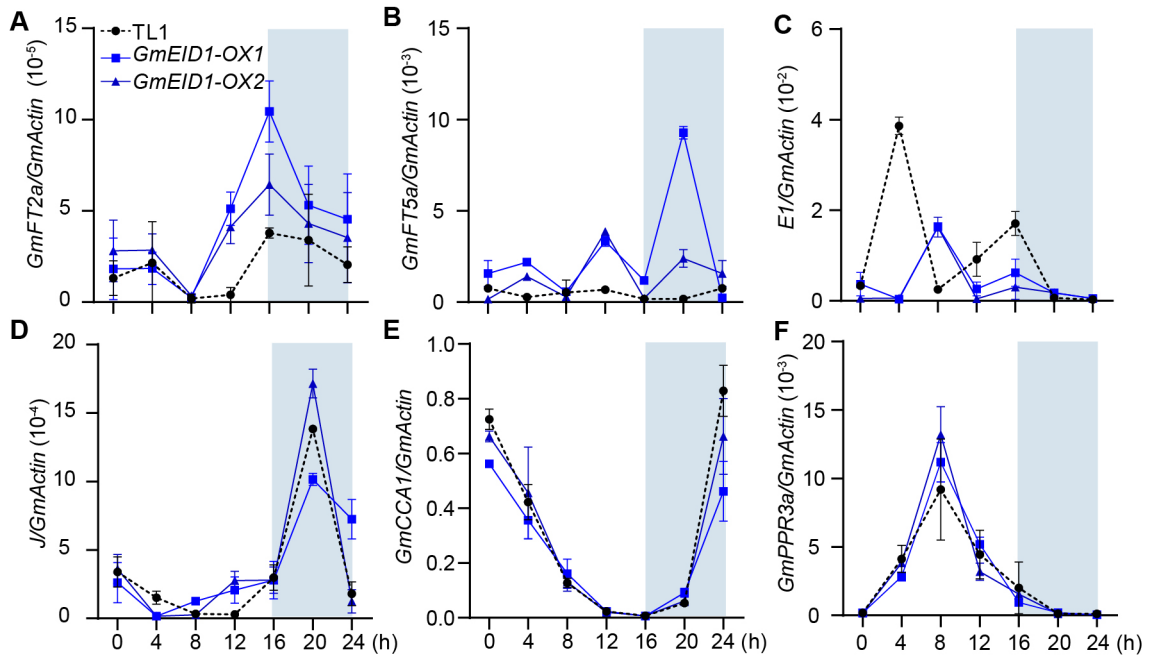


190

191

192 **Fig. S6.** Flowering phenotypes of the *Gmeid1* mutants and *GmEID1-OX* lines. (A and C) Photos
 193 of wild-type TL1, *Gmeid1* mutants and *GmEID1-OX* lines grown under SD conditions (A) or LD
 194 conditions (C) in phytotrons. Scale bar, 10 cm. (B and D) Flowering time of the indicated lines as
 195 in (A) and (C), respectively. (E) Photos of wild-type W82 and *Gmeid1* mutants grown under SD
 196 conditions in phytotrons. Scale bar, 10 cm. (F) Flowering time of indicated lines grown under SD
 197 conditions. The above statistical data are shown as mean values \pm SD ($n = 10$). The lowercase
 198 letters above the dots indicate significant differences ($p < 0.01$, ANOVA with Tukey's post-test).
 199

200

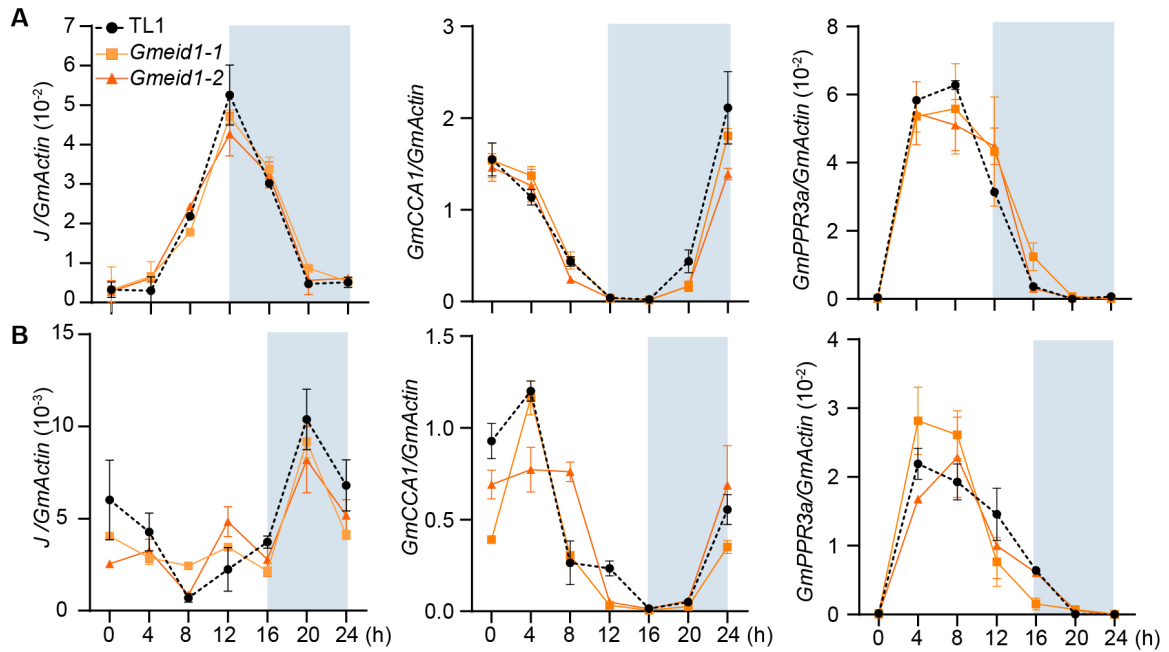


201

202

203 **Fig. S7.** Effects of *GmEID1* overexpression on the transcript levels of the indicated genes.
204 Comparison of the diurnal expression levels of *GmFT2a* (A), *GmFT5a* (B), *E1* (C), *J* (D),
205 *GmCCA1*(E) and *GmPPR3a* (F) in wild-type TL1 and *GmEID1-OX* lines. The second trifoliolate
206 leaves of 20-day-old plants grown under LD conditions were collected for qRT-PCR analysis.
207 Mean values \pm SD (n = 3) is shown. *GmActin* was used as an internal control.

208

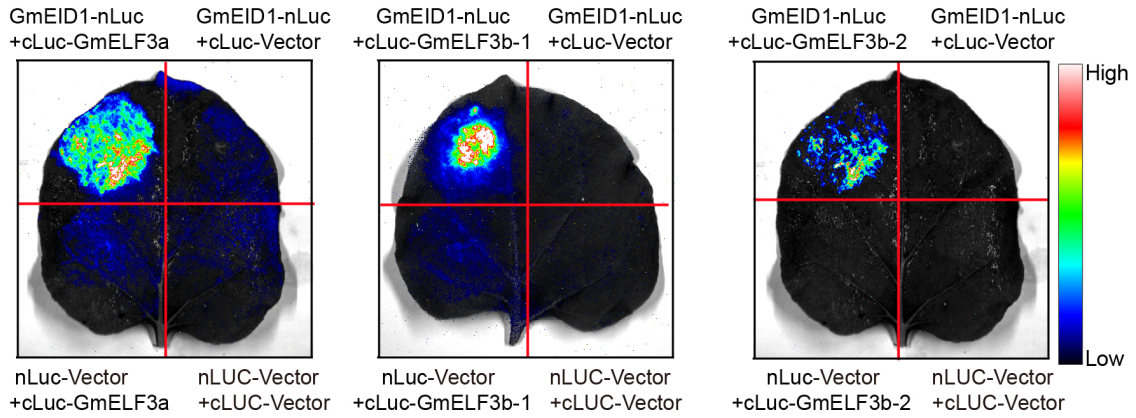


209

210

211 **Fig. S8.** Effects of *GmEID1* mutations on the transcript levels of the indicated genes. Comparison
 212 of the diurnal expression levels of *J*, *GmCCA1* and *GmPPR3a* in wild-type TL1 and *Gmeid1*
 213 mutants under SD conditions (A) and LD conditions (B). The second trifoliolate leaves of 20-day-old
 214 plants were collected for qRT-PCR analysis. Mean values \pm SD ($n = 3$) is shown. *GmActin* was
 215 used as an internal control.

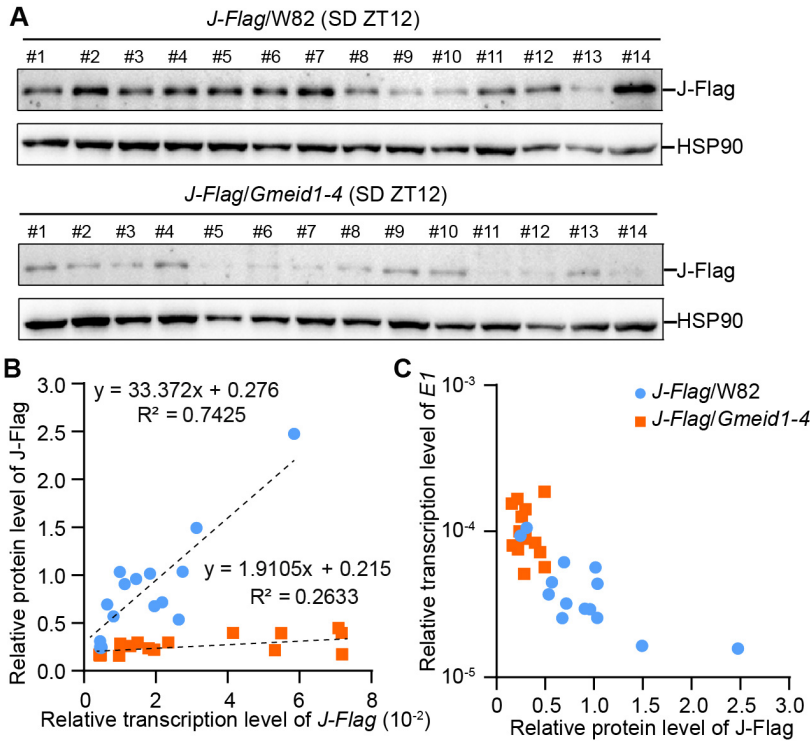
216



217

218 **Fig. S9.** GmEID1 interacts with EC in soybean. Dual-Luciferase assays showing the interaction of
 219 GmEID1 with J, GmELF3b-1 or GmELF3b-2 in tobacco leaves. The empty vector (nLUC-Vector
 220 or cLUC-Vector) was used as a negative control.

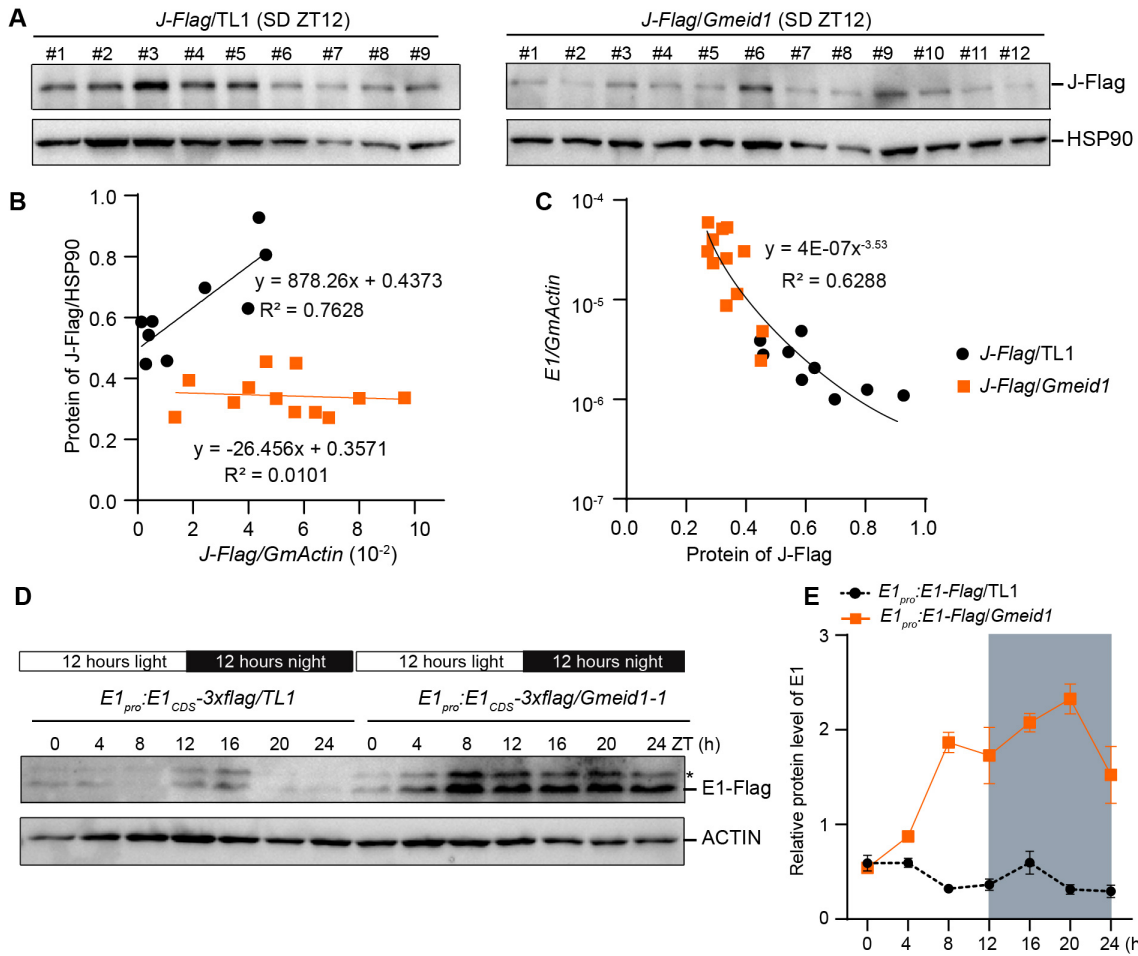
221



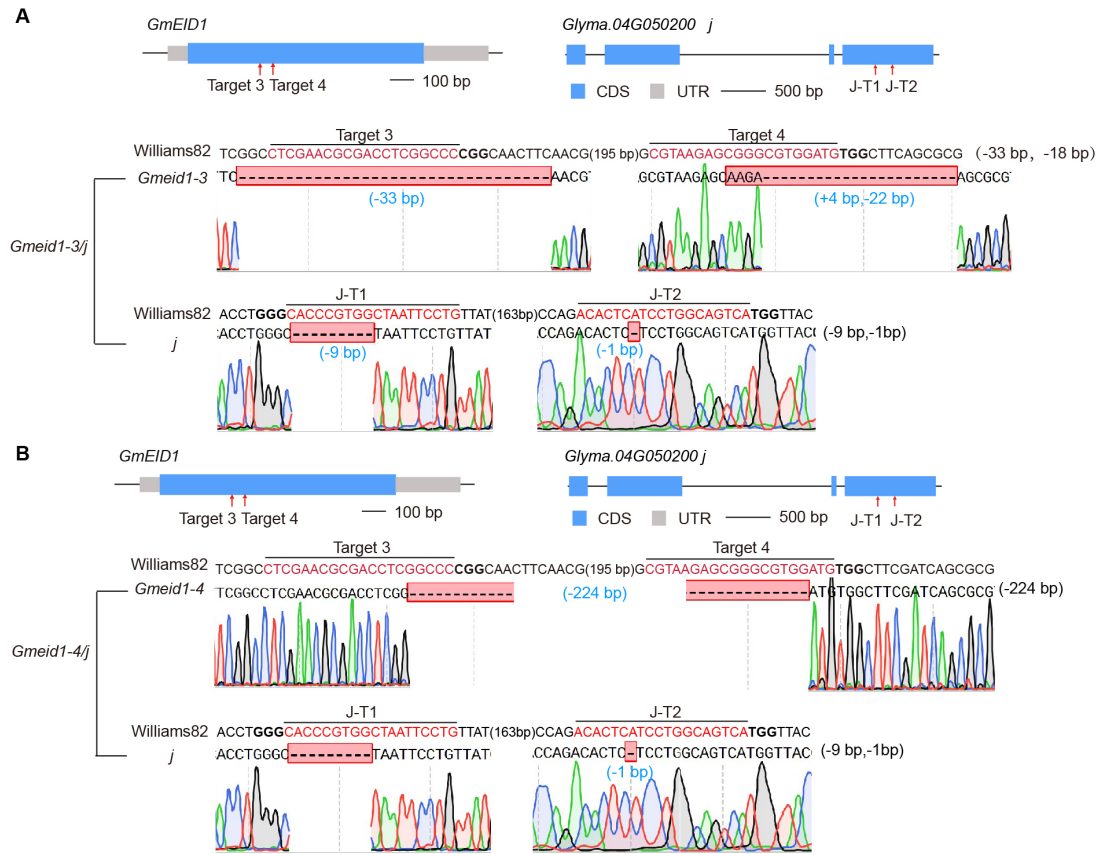
223

224 **Fig. S10.** Analysis of effect of GmEID1 on the abundance of J protein. (A) Immunoblot showing
 225 the abundance of J-Flag protein in the individual root hair callus line harboring transgenic 35S::*J-*
 226 *Flag* in the wild-type W82 background (*J-Flag/W82*, upper panel) or the *Gmeid1-4* mutant
 227 background (*J-Flag/Gmeid1*). Callus lines were cultured under SD conditions and harvested at
 228 ZT12 for immunoblotting using anti-Flag antibody. HSP90 was used as a loading control. (B)
 229 Scatter plot showing the correlation between *J-Flag* transcription levels and protein levels in the
 230 wild-type W82 background and the *Gmeid1-4* mutant background. (C) The correlation between *J-*
 231 *Flag* protein levels and *E1* transcription levels in the callus lines as in (B).

232



235 **Fig. S11.** GmEID1 enhances J abundance and inhibits *E1* transcription. (A) Immunoblot showing
 236 the abundance of J-Flag protein in the transgenic root hair callus cultured under SD conditions.
 237 The *35S::J-Flag* transformed hair root in the wild-type TL1 background (*J-Flag/TL1*, upper panel)
 238 or in the *Gmeid1-1* mutant background (*J-Flag/Gmeid1*) were induced into callus lines. Multiple
 239 transgenic callus lines were harvested at ZT12 for immunoblotting using anti-Flag antibody.
 240 HSP90 was used as the loading control. (B) Scatter plots showing the correlation between the
 241 transcript level and protein level of J-Flag in the wild-type TL1 background and the *Gmeid1-1*
 242 mutant background. (C) The correlation between J-Flag protein level and *E1* transcript level in
 243 TL1 and *Gmeid1-1* mutant callus. (D) Immunoblot showing the protein levels of E1-Flag
 244 expressed by the endogenous *E1* promoter in the TL1 callus and the *Gmeid1* callus during a SD
 245 photoperiod. The membrane was probed by the anti-Flag antibody, stripped, and then probed by
 246 the anti-ACTIN antibody. * Indicates a nonspecific band. (E) Quantitative analysis of E1-Flag
 247 protein levels relative to ACTIN in samples as in (D).

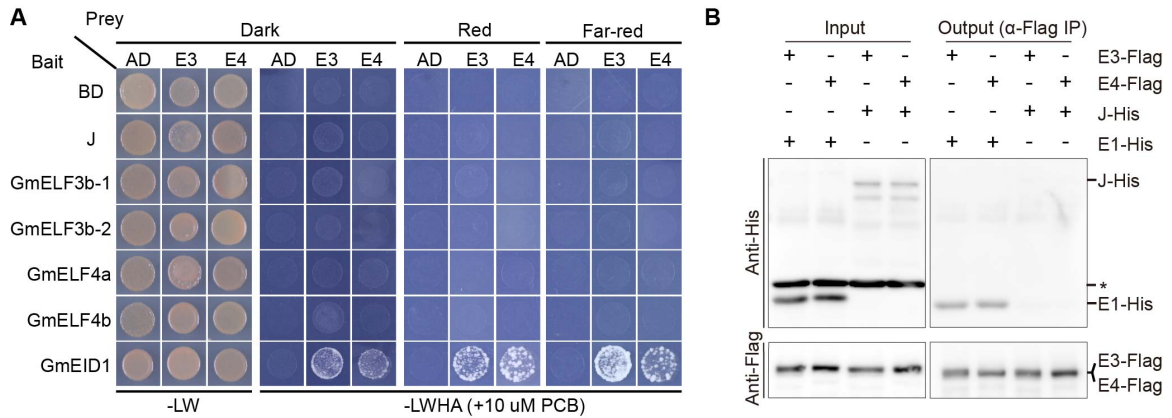


249

250

251 **Fig. S12.** Molecular confirmation of the homozygous progeny of the indicated mutants. (A and B)
 252 DNA sequencing analysis of mutation sites in the *Gmeid1-3/j* double mutant (A) and the *Gmeid1-4/j*
 253 double mutant (B).

254



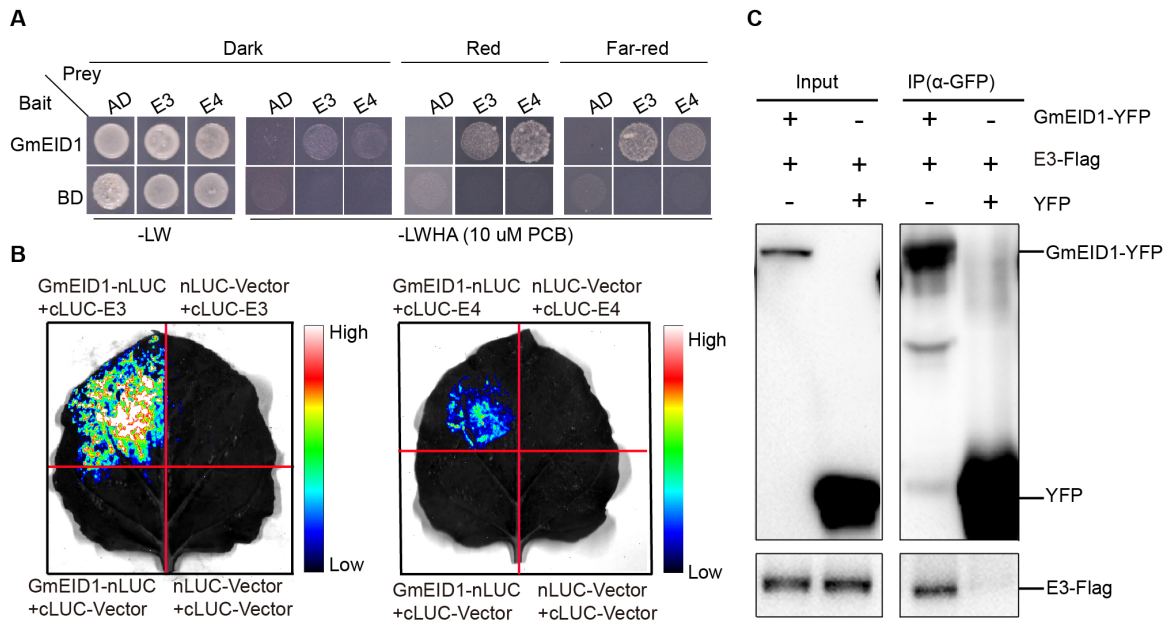
256

257 **Fig. S13.** Investigation of the Interaction between E3/E4 and J. (A) Auxotrophic assay to test
 258 the interactions of indicated protein pairs in yeast cells under red light ($30 \mu\text{mol m}^{-2} \text{s}^{-1}$), far-red
 259 light ($30 \mu\text{mol m}^{-2} \text{s}^{-1}$) or dark conditions. -LW, medium lacking Leu and Trp. -LWHA medium
 260 lacking Leu, Trp, His and Ade. AD, activation domain; BD, binding domain. The interactions
 261 between GmEID1 and E3/E4 were used as positive control. (B) Pull-down assay to test the
 262 interaction between E3/E4 and J protein *in vitro*. E3-Flag, E4-Flag and J-His proteins were
 263 expressed using an *in vitro* translation system. E1-His protein that known interaction with E3
 264 protein was expressed in *Escherichia coli* as positive control. Purified proteins were mixed as
 265 indicated for the pull-down assay. E3-Flag and E4-Flag were detected with anti-Flag antibody,
 266 and E1-His, J-His protein were detected with anti-His antibody. * Indicates a nonspecific band.

267

268

269



270

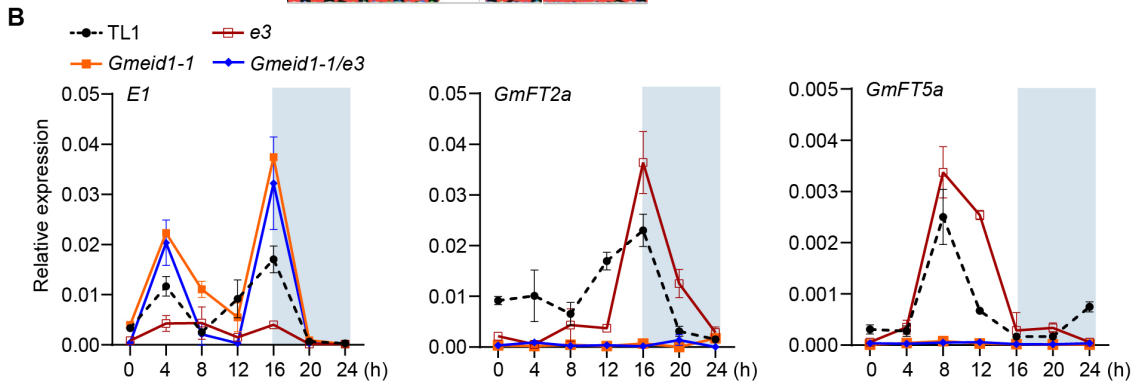
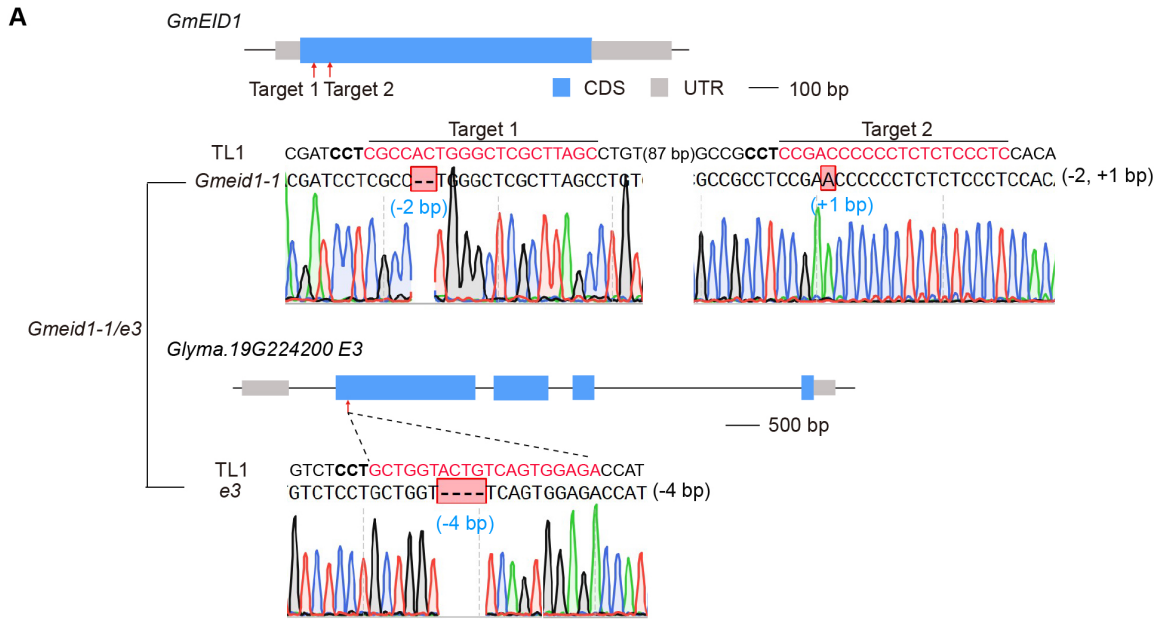
271

272 **Fig. S14.** E3/E4 interact with GmEID1 to inhibit the GmEID1-J interaction. (A) Auxotrophic assay
 273 showing the interaction of GmEID1 with E3/E4 in yeast cells treated with red light ($30 \mu\text{mol m}^{-2} \text{s}^{-1}$),
 274 far-red light ($30 \mu\text{mol m}^{-2} \text{s}^{-1}$) or darkness. Yeast cells (AH109) expressing the indicated
 275 proteins were selected on -LW (lacking Leu and Trp) and -LWHA (lacking Leu, and Trp, His and
 276 Ade) media containing $10 \mu\text{M}$ PCB (phycocyanobilin) under Far-red light ($30 \mu\text{mol m}^{-2} \text{s}^{-1}$) or dark
 277 conditions. AD, activation domain; BD, binding domain. (B) Dual-luciferase assay showing the
 278 interaction of GmEID1 with E3/E4 in tobacco leaves. Empty vector (nLUC-Vector or cLUC-vector)
 279 was used as the negative control. (C) Co-IP assay showing the interaction of GmEID1 with E3.
 280 The indicated constructs (GmEID1-YFP with E3-Flag, and E3-Flag with YFP) were transiently
 281 expressed in tobacco leaves. Total protein extractions (Input) and immunoprecipitation products
 282 prepared by the anti-GFP antibody (IP α -GFP) were fractionated in a SDS-PAGE gel, blotted to
 283 membranes, probed with the anti-GFP antibody (GmEID1-YFP or YFP), stripped, and re-probed
 284 with the anti-Flag antibody (E3-Flag). Empty vector (YFP) was used as the negative control.

285

286

287



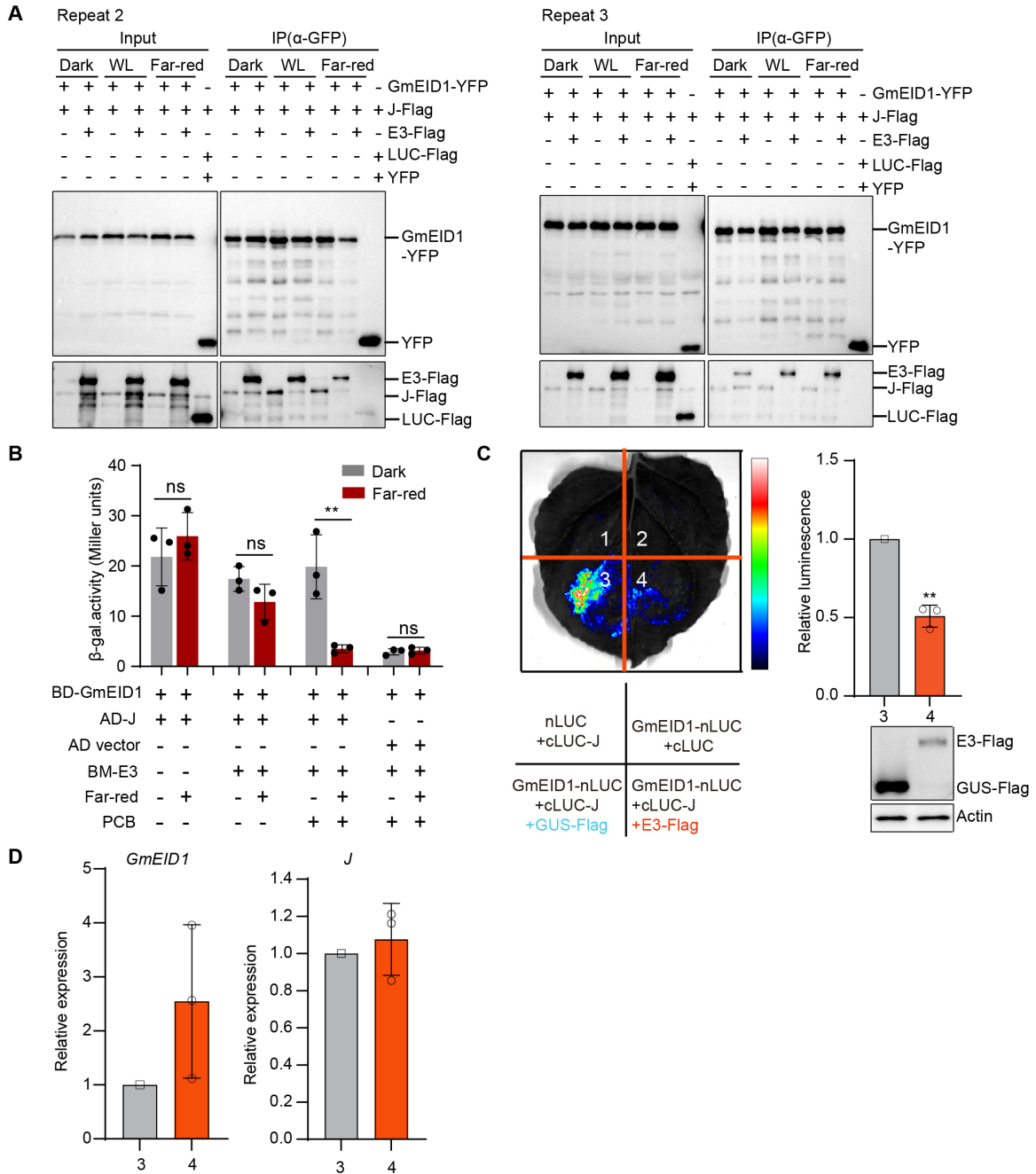
288

289

290 **Fig. S15.** *GmEID1* acts genetically downstream of *E3*. (A) The DNA sequencing analysis to
 291 confirm the genotype of the *Gmeid1-1/e3* double mutant. (B) Diurnal expression levels of *E1*,
 292 *GmFT2a* and *GmFT5a* in the indicated lines. *GmActin* was used as an internal control. Data are
 293 mean \pm SD (n = 3).

294

295



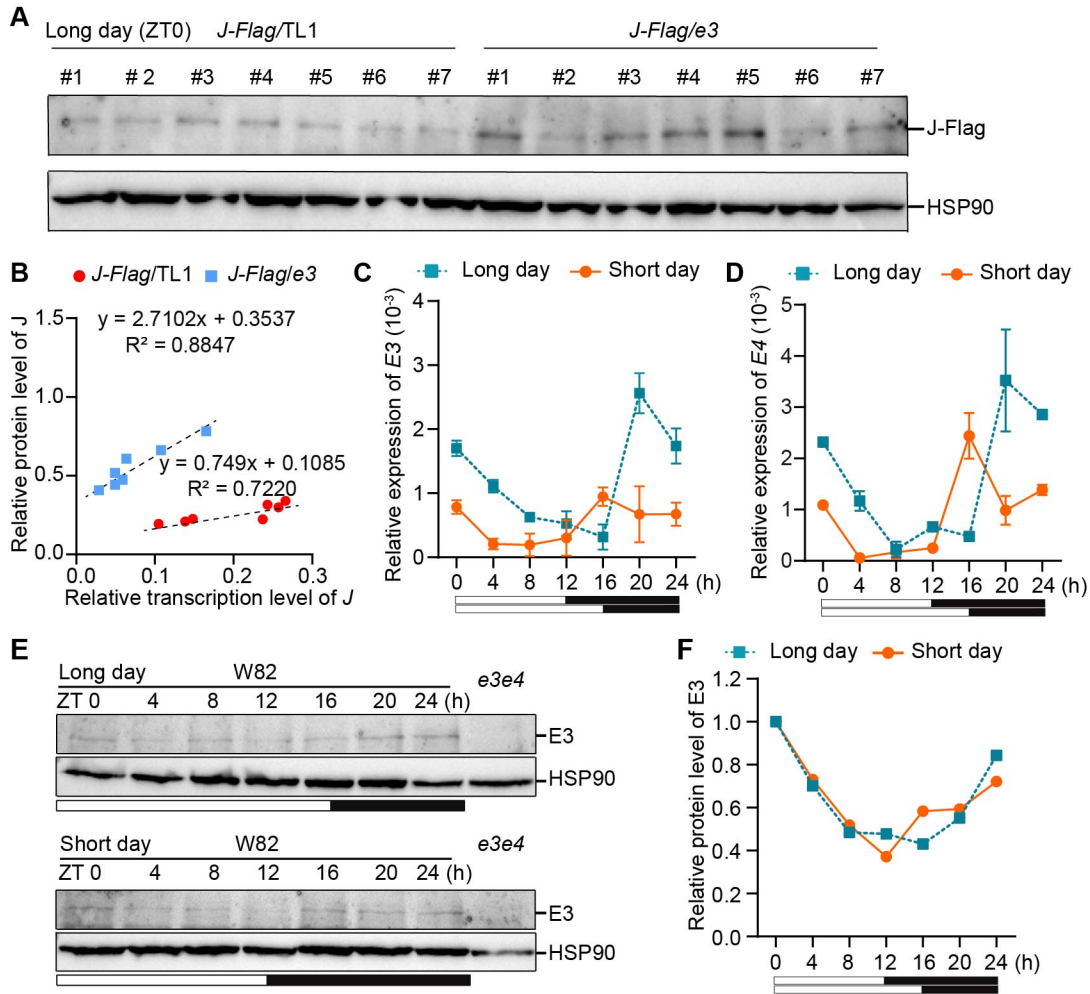
297

298

299 **Fig. S16.** Photo-activated E3/E4 interact with GmEID1 to inhibit the GmEID1-J interaction. (A)
 300 Two biological replicates of Co-IP experiments as in Fig. 4C. (B) Yeast three-hybrid assay to test
 301 the effect of E3 on the interaction between GmEID1 and J. Yeast cells expressing the indicated
 302 proteins were grown in the dark or Far-red ($30 \mu\text{mol m}^{-2} \text{s}^{-1}$) until $\text{OD}_{600} = 0.5-0.8$ for the β -
 303 galactosidase assay. Data are mean \pm SD ($n = 3$). * $p < 0.05$, ** $P < 0.01$, Student's t-test. BD-
 304 GmEID1, AD-J and BM-E3 were expressed by the *pBridge-GmEID1* vector, *pGADT7-J* vector,
 305 and *pBridge-GmEID1-E3* vector, respectively. (C) The indicated constructs were transformed into

306 the tobacco leaves for Dual-luciferase assay. The right panel compared the relative luminescence
307 intensity in the presence of E3-Flag or GUS-Flag which was used as a negative control. Data are
308 mean \pm SD (n = 3). ** $p < 0.01$, Student's t-test. The protein levels of E3-Flag and GUS-Flag in
309 infiltrations 3 and 4 were determined by immunoblot using anti-Flag antibody. Actin was used as
310 the loading control. (D)The *GmEID1* and *J* transcript levels in infiltrations 3 and 4 as in (C) were
311 quantified by qRT-PCR. The *NbActin1* gene was used as the internal control. Data are mean \pm
312 SD (n = 3).

313

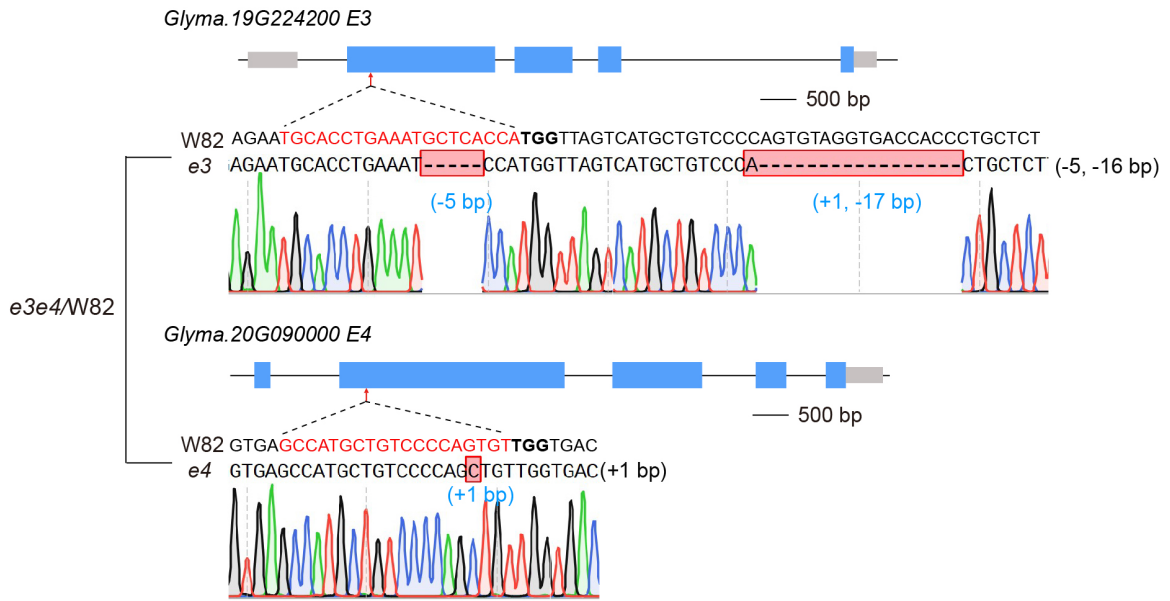


314

315

316 **Fig. S17.** E3 affects the protein levels of J. (A) Immunoblot to compare the J-Flag protein levels in
 317 the indicated root hair callus lines cultured under LD conditions. The *35S::J-Flag* construct was
 318 transformed into the hair root of *e3* mutant in TL1 background (*J-Flag/e3*). Multiple transgenic
 319 callus lines were harvested at ZT0 for immunoblotting using Flag antibody. HSP90 was used as a
 320 loading control. (B) Scatter plot to compare the correlation between transcript levels and protein
 321 levels of transgenic J-Flag in the *e3* mutant and wild-type TL1 as in (A). (C and D) Comparison of
 322 *E3* and *E4* transcript levels in W82 under LD and SD conditions. (E) Immunoblot showing the
 323 protein levels of E3 in W82 under LD and SD conditions using the anti-E3 antibody. The *e3e4*
 324 double mutant was used as negative control. (F) Quantitative analysis of E3 protein levels relative
 325 to HSP90 in the samples as in (E). The values at ZT0 were arbitrarily set to 1.

326

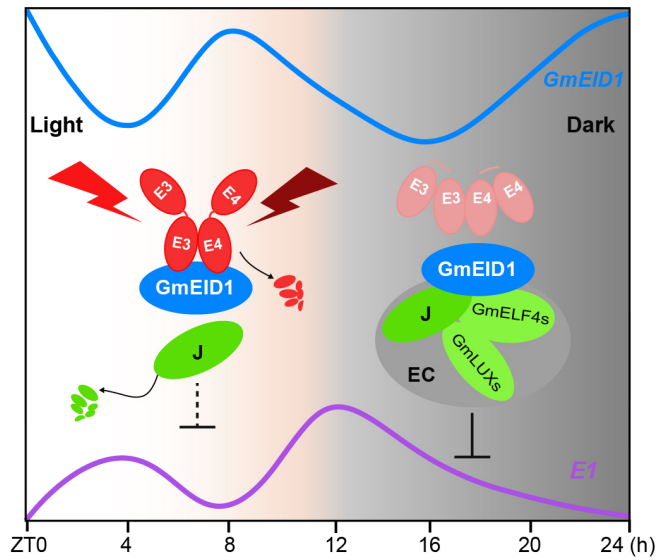


327

328

329 **Fig. S18.** DNA sequencing analysis of mutation sites in the *e3e4* double mutant in W82
330 background.

331

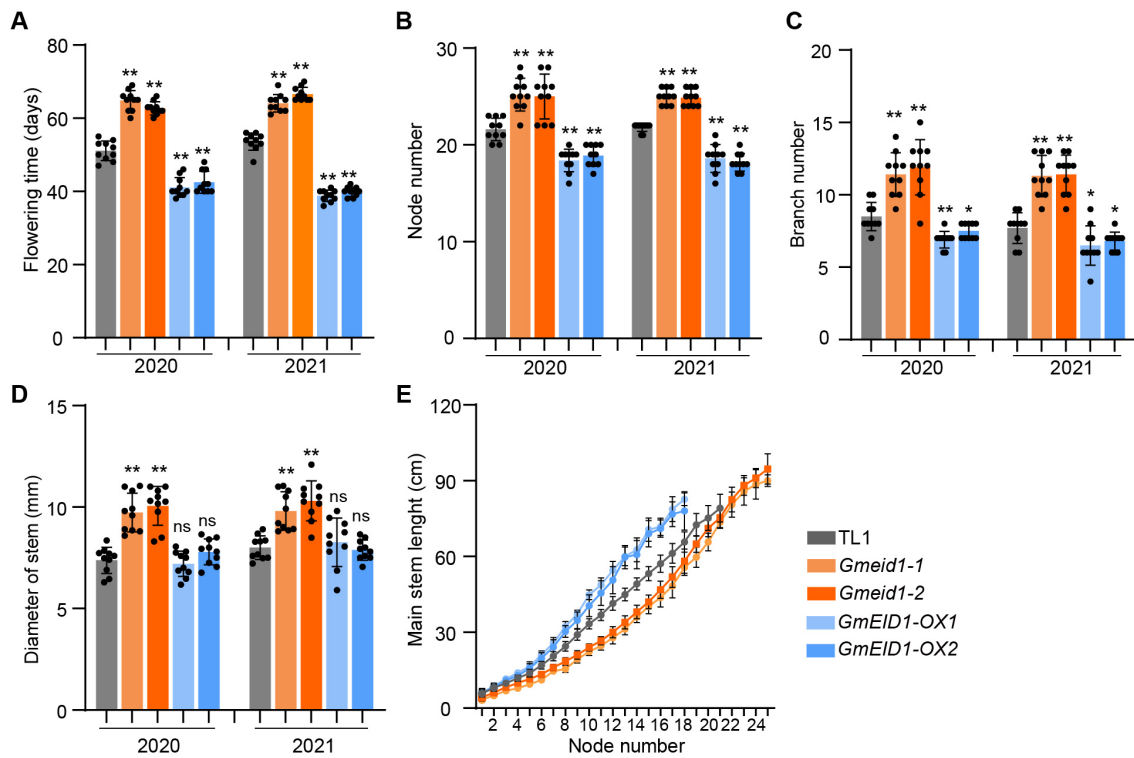


332

333

334 **Fig. S19.** A proposed model illustrating how E3/E4 inhibits the GmEID1-J interaction and
 335 regulates flowering in soybean. During the day, light-activated E3/E4 interacts with GmEID1 to
 336 attenuate the GmEID1-J interaction and promote J degradation. The dark period deactivates
 337 E3/E4, which releases GmEID1 to interact with J. Consequently, J proteins can accumulate and
 338 assemble into EC to inhibit *E1* transcription at night. The blue and purple curves show the
 339 opposite expression patterns of *GmEID1* and *E1* mRNAs, respectively. The *E1* transcript level
 340 rises from the onset of light (ZT0), but slightly decreases during ZT4 to ZT8, which is likely
 341 associated with the light-induced activation and degradation of E3/E4 proteins and the fluctuation
 342 of *GmEID1* transcripts during the light period.

343



344

345

346

347

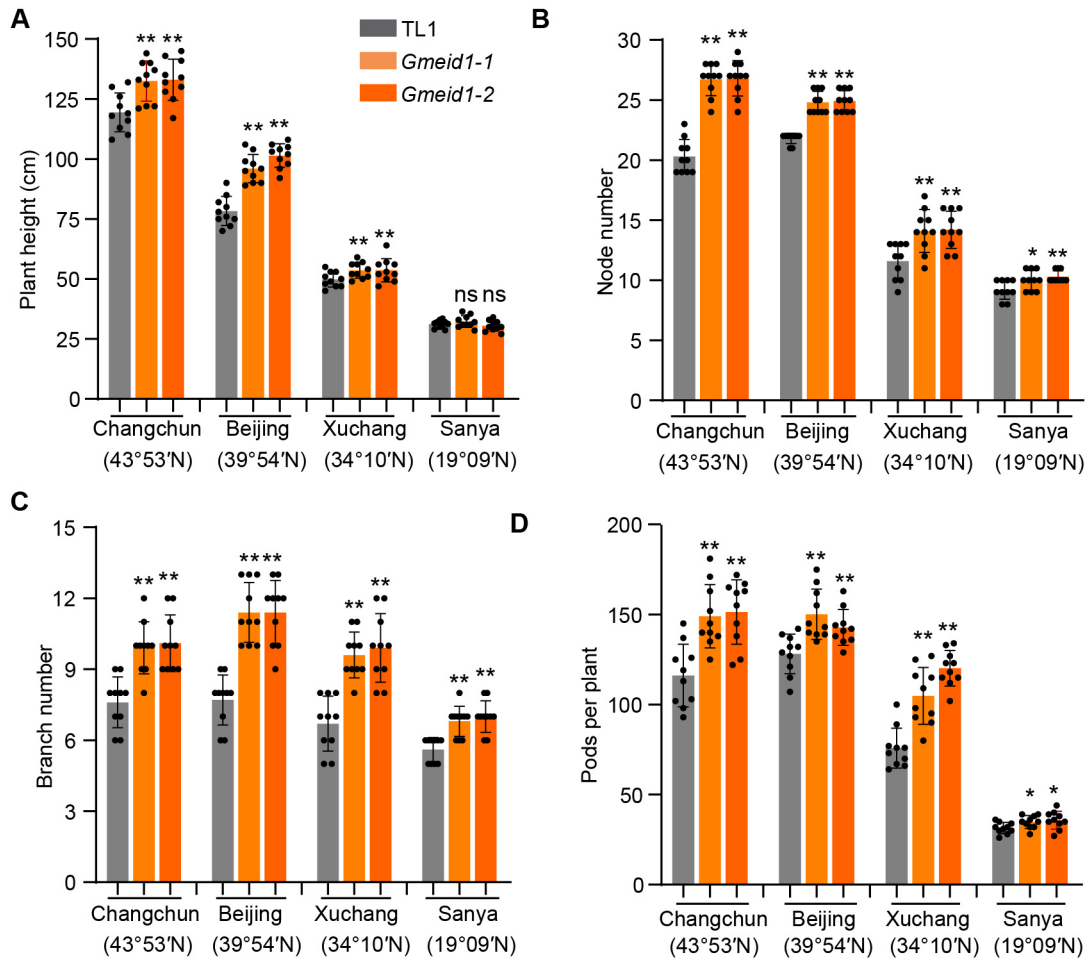
348

349

350

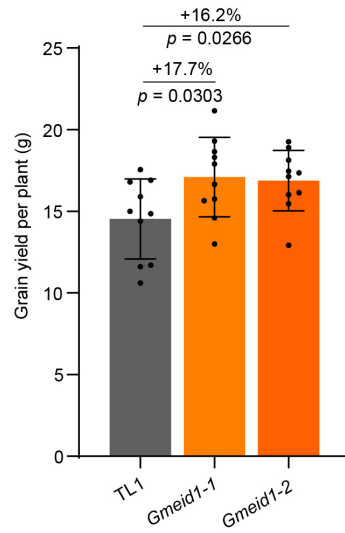
351

Fig. S20. Statistical analysis of the agronomic traits of the indicated lines. (A-D) Comparison of flowering time (A), node number (B), branch number (C) and stem diameter (D) of the indicated lines planted in the Beijing field in 2020 and 2021. (E) The curves of main stem length with each node of the indicated lines in 2021. Above data are means \pm SD ($n = 10$). The significant differences (A-D) were determined by two-tailed Student's t-test ($*p < 0.05$, $**p < 0.01$).



352

353 **Fig. S21.** Statistical analysis of the agronomic traits of the indicated lines at different latitudes. (A-
 354 C) Statistical analysis of plant height (A), node number (B), branch number (C) and pods per
 355 plant (D) of the indicated lines in Changchun (125°19'E, 43°53'N), Beijing (116°23'E, 39°54'N),
 356 Xuchang (104°31'E, 34°10'N) and Sanya (108°56'E, 19°09'N) in 2021. Data are means \pm SD (n =
 357 10) with significant differences determined by two-tailed Student's t-test (* p < 0.05, ** p < 0.01).



358

359 **Fig. S22.** Comparison of yield per plant between the wild-type TL1 and the *Gmeid1* mutants
 360 under normal farming conditions. The indicated lines were grown under a planting density of
 361 about 200,000 plants/hectare in Xuchang in the summer of 2021. Data are means \pm SD (n = 10)
 362 with significant differences determined by two-tailed Student's t-test.

- 363 **Dataset S1 (separate file).** Gene Expression (FPKM) values in second trifoliolate leaves in LD
364 photoperiodic cycle obtained from the RNA-seq experiment.
- 365 **Dataset S2 (separate file).** Screening of candidate regulators of *E1*.
- 366 **Dataset S3 (separate file).** List of primer sequences (5' to 3') used in this study.
- 367 **Dataset S4 (separate file).** Phylogenetic analysis of EID1 and its homologous proteins in the
368 indicated species.
- 369

370
371
372
373
374
375
376
377
378
379
380
381
382
383
384
385
386
387
388
389
390
391
392
393
394
395
396

SI References

1. Y. Naito, K. Hino, H. Bono, K. Ui-Tei, CRISPRdirect: software for designing CRISPR/Cas guide RNA with reduced off-target sites. *Bioinformatics* **31**, 1120-1123 (2015).
2. X. Lyu *et al.*, GmCRY1s modulate gibberellin metabolism to regulate soybean shade avoidance in response to reduced blue light. *Mol. Plant* **14**, 17 (2020).
3. X. Sun *et al.*, Targeted mutagenesis in soybean using the CRISPR-Cas9 system. *Sci. Rep.* **5**, 10342 (2015).
4. A. Kereszt *et al.*, Agrobacterium rhizogenes-mediated transformation of soybean to study root biology. *Nat. Protoc.* **2**, 948-952 (2007).
5. F. Katzen, Gateway((R)) recombinational cloning: a biological operating system. *Expert Opin. Drug Dis.* **2**, 571-589 (2007).
6. M. M. Paz, J. C. Martinez, A. B. Kalvig, T. M. Fonger, K. Wang, Improved cotyledonary node method using an alternative explant derived from mature seed for efficient Agrobacterium-mediated soybean transformation. *Plant Cell Rep.* **25**, 206-213 (2006).
7. S. Chu *et al.*, An R2R3-type MYB transcription factor, GmMYB29, regulates isoflavone biosynthesis in soybean. *PLoS Genet.* **13**, e1006770 (2017).
8. R. M. Galvao *et al.*, Photoactivated phytochromes interact with HEMERA and promote its accumulation to establish photomorphogenesis in Arabidopsis. *Genes & development* **26**, 1851-1863 (2012).
9. X. Lin *et al.*, Novel and multifaceted regulations of photoperiodic flowering by phytochrome A in soybean. *Proc. Natl. Acad. Sci. U.S.A.* **119**, e2208708119 (2022).
10. L. Chen *et al.*, Soybean hairy roots produced in vitro by Agrobacterium rhizogenes-mediated transformation. *Crop J.* **6**, 162-171 (2018).
11. C. Li *et al.*, A domestication-associated gene *GmPRR3b* regulates the circadian clock and flowering time in soybean. *Mol. Plant* **13**, p745–759 (2020).